

## SELF-CEMENTING PROPERTIES AND ALKALI ACTIVATION OF ENEFIT280 SOLID HEAT CARRIER RETORTING ASH

PEETER PAAVER, PÄÄRN PAISTE<sup>\*</sup>, RIHO MÕTLEP,  
KALLE KIRSIMÄE

Department of Geology, University of Tartu, Ravila 14A, 50411 Tartu, Estonia

**Abstract.** *The composition and cementitious properties upon hydration and alkali activation of the solid heat carrier (SHC) ash produced in a new Enefit280 retort was studied. The Enefit280 waste heat boiler (WHB) ash is different from other SHC solid residues. It does not contain residual organics, but is characterized by a low content of reactive Ca-phases and the soluble amorphous (aluminium)-silicate phase/glass material. Cementation of Enefit280 ash upon hydration with plain water is limited and its uniaxial compressive strength stays < 4 MPa after 28 days of curing. Ash mixtures activated with sodium silicate based mixtures show higher compressive strength values, reaching > 10 MPa after 28 days of curing. The Enefit280 ash, compared to other ash types forming in the Estonian oil shale processing industry, has significantly poorer self-cementing properties. This needs to be taken into account when designing waste depositories, if other types of ash with better self-cementing properties are not co-deposited with this ash.*

**Keywords:** *Enefit280 ash, uniaxial compressive strength, ettringite, geopolymer.*

### 1. Introduction

The use of oil shale as a primary fuel in Estonian thermal power plants (TTP) is expected to decrease because of the decommissioning of old pulverized firing (PF) technology boilers, the commissioning of new mixed oil shale and biomass fed power plants, the changing energy markets, and the more stringent environmental regulations. At the same time, the importance of shale oil retorting is increasing and it has been predicted to become the main use of oil shale in the coming decades [1].

Historically, the two main technologies that have been used for producing shale oil in Estonia are the Kiviter process and the Galoter process [2]. The

---

<sup>\*</sup> Corresponding author: e-mail [paarn.paiste@ut.ee](mailto:paarn.paiste@ut.ee)

Kiviter process is conducted in vertical gas generators which are internally heated by the combustion of coke residue and non-condensable shale gas [3]. The solid waste from the Kiviter process is a granular material called semi-coke with an elevated content of residual organics, resulting from incompletely retorted organic matter (up to 10 wt% [4]). The Galoter retorting technology, however, uses spent shale as the heat carrier and is known as solid heat carrier (SHC) technology. The process is based on introducing dried oil shale into an aerofountain drier where it is mixed with hot (590–650 °C) shale ash, produced by the combustion of oil shale semi-coke [5]. The oil yield of 11.5–13% in the Galoter process is ca 3–5% lower than in the Kiviter process, but the advantage of the former is that fine grained and lower calorific value oil shale can be used and the content of unburnt organics is typically below a few percent [6].

Recently, Eesti Energia AS, the largest Estonian oil shale mining and processing company, introduced a new Enefit280 technology that, by its nature, is an enhanced Galoter solid heat carrier retorting system. However, differently from the typical Galoter retort (including similar Petroter retorts operated at Viru Keemia Grupp AS) the retorting unit in Enefit280 is combined with a circulating fluidized bed (CFB) combustion boiler where the spent shale and flue gases are additionally combusted at 800 °C. As a result, the Enefit280 technology is more energy efficient and its overall impact on the environment is smaller, compared to other retorting systems currently in use [7].

The ash content of oil shales is much higher than that in coal – ca 45–50 wt% in Estonian kukersite oil shale, and large amounts of solid waste remain after processing, which must be handled. The composition, physical and chemical properties as well as potential secondary reusability of the oil shale processing wastes depend largely on the composition of the terrigenous matter in the oil shale rock and particularly on the thermal processing regime, either during the burning or retorting. Ca-rich ash, especially its finest fractions, formed at a high temperature (> 1300 °C) in Estonian power plants using PF technology boilers, show strong hydraulic properties and can be used in blends with ordinary cement. The cementitious properties of oil shale ashes generally decrease with decreasing maximum temperatures of oil shale thermal processing, as well as with decreasing time at the peak temperature.

The ash remaining in the Enefit280 system represents a new type of ash material whose behaviour upon hydration (cementation) and potential reusability for synthesising materials used in the building and construction industry is not known. The aim of this contribution is to study the composition of the kukersite oil shale SHC retorting ash remaining at Enefit280 shale oil plants, to evaluate its self-cementing properties when hydrated with plain water, and to assess the development of compressive strength upon alkali activation for potential geopolymer type cement and mortar applications.

## 2. Material and methods

The studied ash was sampled from the Enefit280 type SHC retort and was provided by Eesti Energia AS. The collected ash represented an average ash feed from the waste heat boiler (WHB) system. The cementation and alkali activation of the Enefit280 ash was studied in four series of monolithic samples made by mixing dry ash with the following activators: water, commercial sodium silicate solution with a  $\text{SiO}_2/\text{Na}_2\text{O}$  molar ratio of 2.72, a 5M sodium hydroxide solution, and a sodium silicate and sodium hydroxide mixture with a  $\text{SiO}_2/\text{Na}_2\text{O}$  molar ratio of 1.5. The amount of water used in the mixtures was equal to the maximum water content in fresh ash at pore space saturation conditions, determined experimentally prior to the mixing. Cylindrical specimens of ash/activator mixtures were prepared and stored in PVC tubes under ambient conditions. For each mixture three parallel specimens were made and tested. All sodium silicate based activator solutions were prepared in a way that the added  $\text{Na}_2\text{O}$  to ash ratio in all mix designs was 0.1 (w/w) in order to normalize the amount of added alkali in the mixtures.

The cementing properties of ash mixtures were evaluated by uniaxial compressive strength tests under continuous loading ( $20 \text{ kPa}\cdot\text{s}^{-1}$ ) until failure. Compressive strength was measured in three replicas after 7 and 28 days. The mineral composition of fresh ash and solidified samples was examined using X-ray diffractometry (XRD) on a Bruker D8 Advance diffractometer employing  $\text{CuK}\alpha$  radiation, while the chemical composition was examined using X-ray fluorescence (XRF) analysis on a Rigaku Primus II spectrometer. The scanning electron microscopy (SEM) imaging of test samples was undertaken on a Zeiss EVO MA15 SEM equipped with an Oxford AZTEC energy dispersive X-ray analytical system. The samples were analysed both when uncoated in variable pressure mode and coated with platinum in high vacuum mode. The content of the amorphous glassy phase was estimated by XRD analysis using the ZnO spiked samples. The attenuated total reflectance Fourier transform infrared spectroscopy (ATR-FT-IR) patterns of the mixtures were measured using a Thermo Scientific Nicolet 6700 FT-IR spectrometer at the Institute of Chemistry, University of Tartu.

## 3. Results

### 3.1. Mineral and chemical composition

The mineral composition of the crystalline phases and an amorphous phase of the fresh Enefit280 WHB ash (Fig. 1) is dominated by calcite (44.5 wt%), quartz (8.1 wt%) and K-feldspars (7.7 wt%). The content of dolomite is on average 1.0 wt%. All these components represent the inherited sedimentary mineral phases that are characteristic of raw oil shale. In addition, the WHB

ash contains secondary phases formed during the thermal treatment of oil shale – authigenic Ca-silicates (11.2 wt%) and periclase (1.0 wt%), but it is low (< 2%) in free CaO (lime).

The chemical composition of the fresh WHB ash corresponds to its mineral composition and is dominated by SiO<sub>2</sub> and CaO that on average make up 25.5 and 30.22 wt%, respectively (Table). The level of MgO, Al<sub>2</sub>O<sub>3</sub> and Fe<sub>2</sub>O<sub>3</sub> in the fresh ash is on average 1.95, 11.13 and 4.83 wt%, respectively. The content of SO<sub>3</sub> varies between 1.5 and 4.2 wt% with an average of 3.97 wt%.

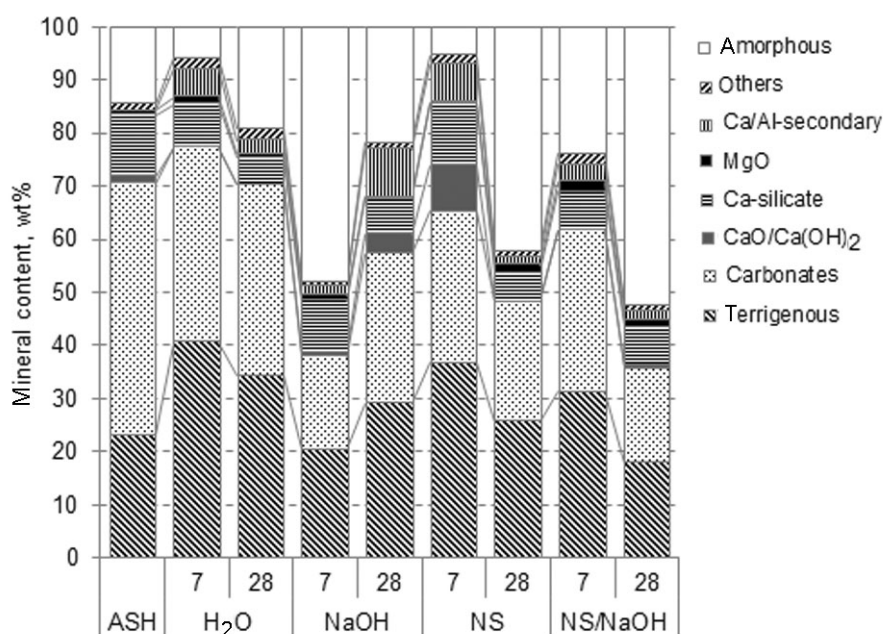


Fig. 1. Mineral composition of the WHB ash and mixtures with activators over 7 and 28 days of curing. Terrigenous minerals – quartz, K-feldspar, K-mica; carbonate minerals – calcite, vaterite, dolomite; CaO/Ca(OH)<sub>2</sub> – lime, portlandite; Ca-silicate – C<sub>2</sub>S, merwinite, wollastonite; Ca/Al-secondary – ettringite, hydrocalumite; others – magnetite, hematite, gypsum, anhydrite.

**Table. Chemical composition of the original WHB ash and the mixtures after 28 days of curing**

Mixture	SiO <sub>2</sub>	Al <sub>2</sub> O <sub>3</sub>	TiO <sub>2</sub>	Fe <sub>2</sub> O <sub>3</sub>	MnO	CaO	MgO	Na <sub>2</sub> O	K <sub>2</sub> O	P <sub>2</sub> O <sub>5</sub>	SO <sub>3</sub>	L.O.I.	SUM
Fresh WHB ash	25.5	11.13	0.49	4.83	0.06	30.22	1.95	0.09	3.51	0.11	3.97	17.65	99.51
H <sub>2</sub> O	24.33	10.28	0.52	4.79	0.04	28.94	1.86	0.09	3.3	0.12	3.79	21.39	99.45
5M NaOH	22.46	9.64	0.43	4.25	0.06	26.53	1.72	5.38	3.06	0.1	3.5	22.11	99.24
NS	29.91	9.11	0.41	3.66	0.07	24.87	1.65	7.16	2.93	0.09	3.28	17	100.14
NS/NaOH	27.9	9	0.37	3.93	0.05	24.55	1.59	9.85	2.82	0.08	3.23	16.94	100.31

The mineral and chemical compositions of the WHB ash and water mixtures are different from those of the fresh ash because of hydration and carbonation reactions taking place during the curing process (Fig. 1, Table). The major difference in the mineral composition between the hydrated samples after 7 days is the disappearance of CaO and the portlandite  $\text{Ca}(\text{OH})_2$  phase, as well as the formation of a secondary Ca-Al hydrate phase hydrocalumite and a hydrous Ca-Al sulfate phase ettringite. The contents of hydrocalumite and ettringite after 7 days are 3.7 and 1.4%, respectively. There is also a change in the amorphous phase. The level of the amorphous phase in the fresh ash is about 14 wt% and in the 7-day-old sample about 6 wt%. This might indicate that some part of the X-ray amorphous phase is dissolved and recrystallizes into a crystalline phase, in our case, hydrocalumite and ettringite. However, after 28 days hydrocalumite has practically disappeared and the relative content of the amorphous phase shows an increase, indicating that the metastable phases including the Ca-silicate phases and hydrocalumite have started to decompose, possibly forming a (semi)-amorphous calcium-silica-hydrate (C-S-H) phase.

The evolution of the mineral composition of the samples treated with the NaOH activator is different from that of the samples mixed with plain water. There is no ettringite detected in the NaOH activated mixtures and hydrocalumite is present in the samples cured for 28 days. Regarding the chemical composition, the major difference between the fresh ash and 28-day-old NaOH-water mixtures is the increase in  $\text{Na}_2\text{O}$  in the latter, which is due to the addition of NaOH (Table). Similarly to the ash-water mixtures the NaOH samples also show an increase in the loss on ignition (L.O.I.) values, which is possibly due to the carbonation of portlandite.

The mineral composition of the WHB ash specimens made of mixtures with sodium silicate based solutions differs considerably from that of the samples treated with water or NaOH. A major difference between the fresh ash and water and NaOH mixed samples is in the amorphous phase content, which, differently from the constant 14 wt% in the former, varies from 6 to 52 wt% in the samples mixed with Na-silicate, depending on its amount added (Fig. 1). This is evidently due to recrystallization reactions and most importantly the formation of an amorphous Ca-Na-Al-silicate gel in the reaction between the Na-silicate solution and the minerals present in the WHB ash. It seems that the reaction with the Na-silicate solution starts to use up the Ca from the dissolution of Ca-carbonate phases, indicating the formation of an amorphous C-S-H phase. There are no significant mineralogical differences between the samples activated by Na-silicate and those treated with Na-silicate + NaOH solutions. The differences in mineral composition between these two mixtures vary in the range of a few percent (Fig. 1), indicating similar changes in both mixtures. The observed changes in the chemical composition of the Na-silicate and Na-silicate/NaOH mixtures, when compared to the original fresh ash, are related to the addition of Na and Si. In the samples mixed with Na-silicate the level of  $\text{SiO}_2$  has

increased to 27.90 wt% in the sample prepared with Na-silicate + NaOH and to 29.91 wt% in the sample prepared with only Na-silicate (Table).

### 3.2. Attenuated total reflectance Fourier transform infrared spectroscopy

Attenuated total reflectance Fourier transform infrared (ATR-FT-IR) spectra of the initial ash and activated samples after 7 and 28 days are shown in Figure 2. All spectra are characterized by bands at around  $1410\text{ cm}^{-1}$  representing the C–O stretch,  $873\text{ cm}^{-1}$  corresponding to the C–O out-of-plane bend and a  $712\text{ cm}^{-1}$  band representing the C–O in-plane bend in the  $\text{CO}_3^{2-}$  ion [8, 9], which show the presence of calcite (and dolomite), also detected in the XRD analysis. The shoulder at  $1120\text{ cm}^{-1}$  and the low-intensity band at  $594\text{ cm}^{-1}$  in the original ash spectrum correspond to the stretching and bending of the S–O bond in the  $\text{SO}_4^{2-}$  ion in the sulfate bearing phases (ettringite) [9]. The bands indicating Si functional groups in silicate mineral phases in the original ash appear between  $400$  and  $1200\text{ cm}^{-1}$ . In the activated samples, as opposed to the original ash, the changes in the ATR-FT-IR spectra occur. New bands at around  $3300\text{--}3400\text{ cm}^{-1}$  and  $1640\text{ cm}^{-1}$ , corresponding to O–H stretching and bending vibrations of water, form in all activated samples due to hydration. In addition, a sharp band at  $3640\text{ cm}^{-1}$ , which is characteristic of the O–H stretching in portlandite  $\text{Ca}(\text{OH})_2$ , is present [10]. The activation of Si phases is indicated by the shifts of the Si–O–Si (Si–O–Al) band, representing asymmetric stretching vibrations in  $\text{SiO}_4$  tetrahedra [11]. In the water-ash mixtures this band shifts to higher wavenumbers after 28 days of curing, indicating polycondensation of silicate species and longer silicate structures encompassing more silica tetrahedra in the  $\text{Q}^2$  configuration. The broad band at  $1110\text{ cm}^{-1}$  can be interpreted as a combination of Si–O stretching vibrations from amorphous silicate phases associated with branching  $\text{Q}^3$  silicon sites [12] and S–O vibrations of  $\text{SO}_4^{2-}$  in sulfate minerals. The NaOH activated ash mixtures (Fig. 2a–b) show a Si–O–Si (Si–O–Al) asymmetric stretching vibrations band that after 7 days of curing splits into two components at ca  $930\text{ cm}^{-1}$  and ca  $980\text{ cm}^{-1}$ . These can be interpreted as Si–O–Al and Si–O–Si stretching vibrations in  $\text{Q}^2$  (1Al) and  $\text{Q}^2$  silicon sites, respectively [13]. The well-defined shape of the  $930\text{ cm}^{-1}$  band indicates a crystalline silicate structure. Its disappearance after 28 days of curing suggests that a reaction period longer than 7 days should be needed for the NaOH activation in order to depolymerise the initial silicate structure. An excess of Ca compared to Si in the C-S-H gel formation is evident from the secondary portlandite formation, corresponding to the sharp band at  $3640\text{ cm}^{-1}$ .

The ATR-FT-IR spectra of the WHB ash and the sodium silicate based mixtures (Fig. 2a–b) show a Si–O–Si (Si–O–Al) stretching band shifting to lower values of around  $960\text{ cm}^{-1}$  after 7 days and then back to higher values of  $970\text{--}980\text{ cm}^{-1}$  after 28 days, depicting the initial depolymerisation and

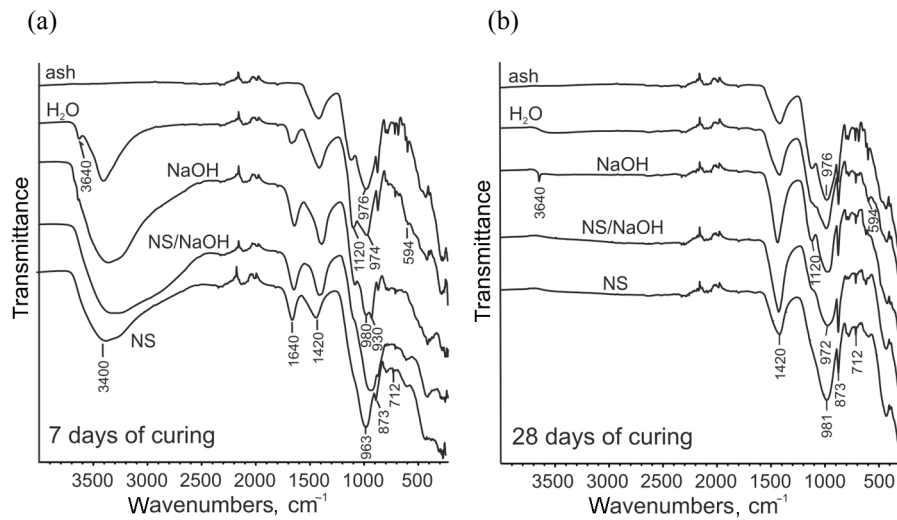


Fig. 2. ATR-FT-IR spectra of the studied ash and mixtures after 7 (a) and 28 (b) days of curing.

subsequent rearrangement of silicate bonds back into polymeric chains. The shift towards a higher wavenumber corresponds to longer and more interconnected polymeric silicate species [13]. Interestingly, the spectrum recorded after 7 days of curing shows that the Si–O–Si peaks have shifted to lower wavenumbers than in the spectra recorded for the H<sub>2</sub>O activated ash. This corresponds to the findings of a previous study [12], showing that the higher Na<sup>+</sup> content leads to the Si–O–Si band shifting to lower wavenumbers.

### 3.3. Microstructure

The scanning electron microscope (SEM) analysis of the original WHB ash shows that the material is fine grained with a particle size generally less than 100  $\mu\text{m}$ , while fine particles with a diameter of ca 20  $\mu\text{m}$  predominate (Fig. 3a). The particles are irregular in shape and the finest particles are somewhat aggregated into lumps of 20–30  $\mu\text{m}$  in size (Fig. 3b). The samples mixed with water (Fig. 3c) show recrystallization and development of secondary Ca–Al and Ca–Al-sulfate minerals in the material pore space. The ash particles are covered by secondary precipitates and the bonds between the particles are generated by interlocking needle- and lath-shape authigenic minerals. Their crystallite morphology and chemical composition identify them as hydrocalumite and ettringite, even though the relative abundance and particularly the size of the lath- and needle-like ettringite crystallites are much smaller than those observed in other hydrated oil shale ashes [14].

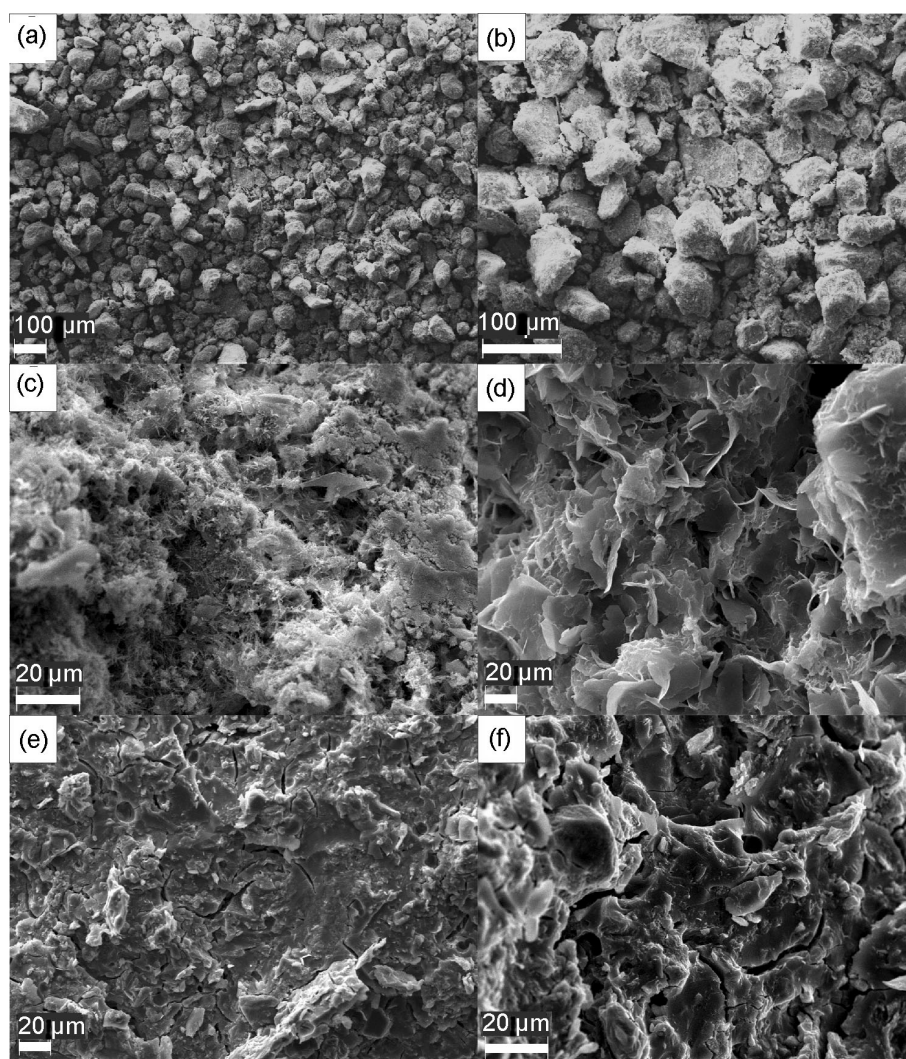


Fig. 3. SEM electron images of the Enefit 280 WHB ash and mixtures after 28 days of curing: (a), (b) unhydrated ash; (c) ash and water mixture; (d) ash and 5M NaOH mixture; (e) ash and Na-silicate mixture; (f) ash and Na-silicate/NaOH mixture.

The mixtures activated only with the NaOH solution show a similar microstructure to the water mixed samples (Fig. 3d), but their pore-space is filled with hydrocalumite platy crystals and crystal aggregates while no lath-shape ettringite crystals are detected. This finding correlates well with the mineralogical analysis showing the absence of ettringite and the presence of abundant hydrocalumite in the ash-NaOH system. The size of the hydrocalumite crystallites is generally 2–5 μm. Being similar to each other, the microstructures of Na-silicate/NaOH and Na-silicate activated mixtures considerably differ from that of water and NaOH mixtures (Fig. 3e–f). Under

SEM the energy dispersive analysis of the material shows that it is composed of a Ca-Na-Al-silicate gel-like matrix that is completely filling the area between the unreacted ash particles. This agrees with the higher amount of the amorphous phase revealed in the XRD analysis of these mixtures.

### 3.4. Uniaxial compressive strength

The average uniaxial compressive strength of the Enefit280 WHB ash and plain water mixtures after 7 days of curing was about 3.5 MPa. This value did not improve much after 28 days of curing, remaining 3.8 MPa on average (Fig. 4). In contrast, the WHB ash samples mixed with the sodium silicate solution and the ash mixed with the Na-silicate/NaOH solution achieved typically quite high compressive strength values already after 7 days of curing (Fig. 4). However, after 28 days of curing the samples mixed with Na-silicate did not gain any additional strength, which was even lower on average. Compared to water and pure sodium silicate mixtures, the samples mixed with the Na-silicate + NaOH solution exhibited a significantly higher compressive strength. All samples gained strength over the curing period and after 28 days of curing they attained a compressive strength of 10 MPa on average. The samples prepared with only the NaOH solution did not gain any significant strength over the curing period between 7 and 28 days and a compressive strength of only 1 MPa was achieved after the 28 day curing period.

After 7 and 28 days of curing under ambient conditions the compressive strength curves of the Enefit280 WHB ash and plain water mixtures (Fig. 5a–d) are characterized by the brittle behaviour of the material,

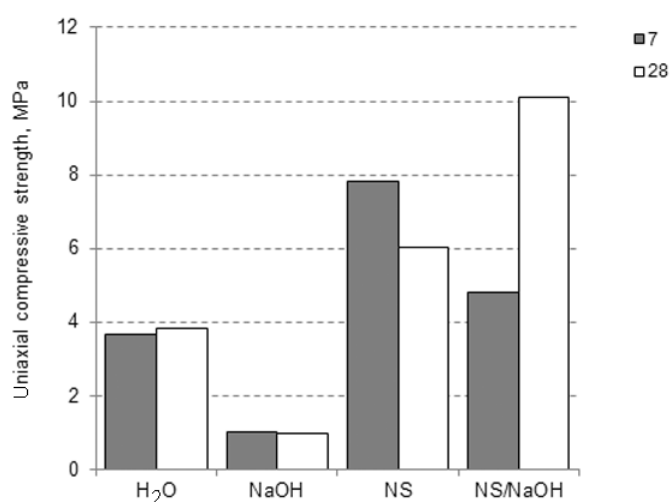


Fig. 4. Uniaxial compressive strength of samples mixed with different activators after 7 and 28 days of curing. H<sub>2</sub>O – water; NaOH – 5M sodium hydroxide; NS – Na-silicate; NS/NaOH – Na-silicate and sodium hydroxide mixture.

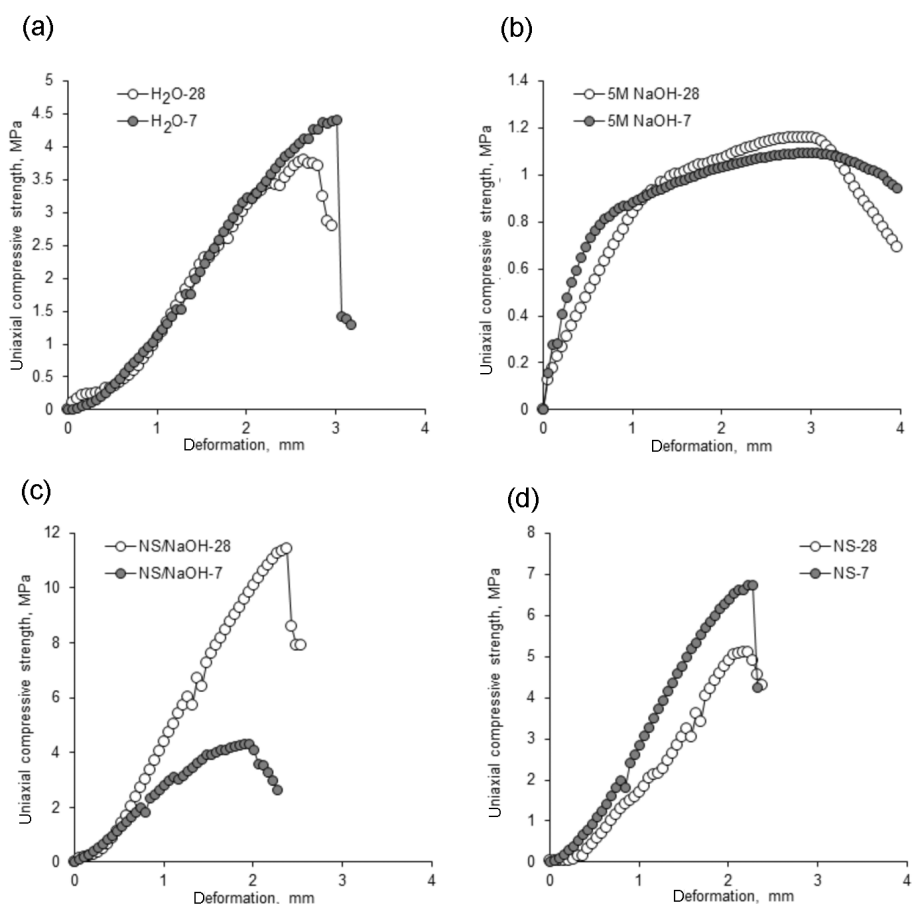


Fig. 5. Compressive strength curves of WHB ash mixtures after 7 and 28 days of curing: (a) ash and water mixture; (b) ash and 5M NaOH mixture; (c) ash and Na-silicate mixture; (d) ash and Na-silicate/NaOH mixture.

whereas there is little difference between the final compressive strength values achieved after 7 and 28 days. In contrast, different compressive strength curves and development of the compressive strength were observed in the samples activated with the high molar NaOH activator (5M NaOH). After 7 and 28 days of curing the material showed high residual strength (“elastic” behaviour) and plastic/ductile deformation (Fig. 5a–d), indicating that no rigid cementation was developed. The Na-silicate and Na-silicate/NaOH activated samples show a remarkably different behaviour compared to the mixtures made with plain water and the NaOH activated samples (Fig. 5a–d). Both mixtures exhibit high strength values and a characteristic brittle behaviour already after 7 days of curing, this property being visible after 28 days as well.

#### 4. Discussion

The composition of the Enefit280 ash is significantly different from that of the other retorting residues produced either in the Kiviter-type retorts (semi-coke) or other SHC Galoter-type retorts, including Petroter and Enefit140 (black ash). Firstly, the residues from the latter are black/dark grey in colour due to the presence of unburnt organic carbon ( $C_{org}$ ) whose content varies between 1.5 and 2.2 wt% in the Petroter ash [15] and from 8 to 10 wt% in semi-coke [4], whereas the Enefit280 ash is grey-beige and does not contain any significant amount of residual organic carbon. This is due to the effective carbon burnout during the waste processing in the CFB furnace in the Enefit280 retorting system. The solid residues from the retort are kept in the presence of excess oxygen at temperatures of about 800 °C, to allow a burnout of all organics left in the material after retorting. In addition to the absence of residual organics the CFB boiler attached to the Enefit280 retort ensures efficient high temperature conversion of the mineral material in the presence of oxygen. As a result, the Enefit280 WHB ash does not contain a CaS (oldhamite) phase. Oldhamite is particularly characteristic of retorting residues [4, 16], but does not occur in thermal power plant ashes [17, 18]. Oldhamite forms under oxygen deficiency conditions in the reaction between CaO and SO<sub>2</sub>. Another mineral indicating oxygen deficiency in the retorting process is a partly oxidised Fe-oxide mineral magnetite Fe<sub>3</sub>O<sub>4</sub> (FeO·Fe<sub>2</sub>O<sub>3</sub>) in older SHC ashes, whereas in the WHB ash like TPP ashes the hematite Fe<sub>2</sub>O<sub>3</sub> is typically present [16].

In this sense the Enefit280 WHB ash is considered to be similar to TPP ashes, particularly to these formed in CFB boilers. However, the mineral characteristics of the WHB ash indicate that the content of several reactive phases (e.g. lime, belite-C<sub>2</sub>S) that can potentially react with water and are therefore responsible for hydraulic self-cementing, is low when compared to the Petroter ash or any other TPP ashes [15, 17, 19]. For example, the content of belite, which is a typical phase in a cement clinker with a final compressive strength of about 40 MPa for a pure compound [20], is rather low (< 4 wt%) in the WHB ash. In addition, the content of other secondary Ca-silicates (merwinite, wollastonite and akermanite) is remarkably lower (< 12% in total) than in other oil shale ashes [17]. Importantly, the Enefit280 WHB ash contains a notably low amount (< 3%) of lime CaO and/or portlandite Ca(OH)<sub>2</sub>, suggesting that carbonation reactions do not contribute much to the stabilization of the sediment either.

Moreover, the formation of the secondary Ca-Al-sulfate hydrate phase (ettringite) and Ca-Al-phase (hydrocalumite), a characteristic process in hydrated oil shale ash and semi-coke deposits [4, 14, 18, 21, 22], is subdued in the Enefit280 WHB ash. Ettringite formation requires the presence of soluble Ca, Al and sulfate [23]. The sulfate needed for ettringite formation could be delivered by dissolution of the anhydrite CaSO<sub>4</sub>. However, due to an overall low content of sulfate and a low content of CaO/portlandite the

amount of ettringite measured in the water treated samples was rather low (max 2 wt%). In comparison, the hydration of oil shale ash from thermal power plants and the semi-coke waste from shale oil retorting typically results in a high ettringite content, reaching 30 wt% of crystalline phases [4]. A similar low content of ettringite upon hydration with water was observed in the Petroter ash where ettringite was nearly absent [16] or was found to occur in a low content, < 5 wt% [15]. Ettringite plays an important role in the self-cementing properties of oil shale ash and semi-coke deposits by forming interlocking meshes of needle-like crystals filling the pores space [22]. This suggests, judging only by the phase composition of the WHB ash, that the uniaxial compressive strength values developing upon simple hydration of this ash type are low compared to ash stone formed from other Estonian oil shale ashes [24]. This prediction of limited self-cementing properties of the Enefit280 WHB ash is further supported by the uniaxial compression tests of the WHB ash mixtures with plain water, showing an average compressive strength value of about 3.5 MPa after 7 days of curing under ambient conditions and an average of 3.8 MPa after 28 days. In comparison, the ash from pulverized firing boilers reaches a compressive strength value > 10 MPa, the CFB ash > 7 MPa [19] and the Petroter SHC ash > 5 MPa [15] in the same period of time.

Surprisingly, the alkali activation of the Enefit WBH ash with the NaOH solution, aimed to promote (geo-)polymerization [25], resulted in a lower final compressive strength than in the water mixed ash samples. There is no ettringite observed in the XRD nor in the SEM analysis of the NaOH treated samples and it is possible that the low compressive strength values of the samples activated with NaOH, specifically after the 7-day curing period, are due to the absence of needle-like ettringite and/or Ca-monosulfate crystallites that in the ash-water mixtures start to form rigid bridges between the ash particles. At high molar concentrations of the NaOH solution where pH ca 14 is maintained, the ettringite formation depends on the activity of calcium in the solution while the formation of calcium hydroxide and sodium-substituted monosulfate phase competes with ettringite formation [26]. In the Enefit280 ash systems it is evident that due to the low presence of soluble Ca minerals the activity of Ca is high and that with addition of a strong NaOH solution the ettringite precipitation is suppressed, resulting instead in the formation of hydrocalumite and possibly some amorphous gel-like material, as is evident from the ATR-FT-IR data. However, this gel and the platy crystals of the dominant cementitious secondary mineral hydrocalumite do not provide a similar interlocking and an overall strength as the ettringite meshes. Similar effects were observed by Paaver et al. [15] in Petroter ashes treated with the NaOH solution.

Geopolymerization with the formation of a Ca-Al-Si amorphous matrix and the development of high compressive strength is evident in the Na-silicate and Na-silicate/NaOH activated samples. As a result, the behaviour of these samples is remarkably different from that of the ash and water

mixture as well as the NaOH activated samples. Both of the sodium silicate containing mixtures show higher strength values, exceeding 10 MPa. The relatively good compressive strength established in these mixtures is evidently provided by the Ca-Na-Al-silicate gel formation in the pore space of the ash aggregate, as is observed in the SEM, XRD and ATR-FT-IR analyses. The latter also shows the occurrence of depolymerization-repolymerization processes of silicate phases in these mixtures.

High-Ca ashes like the Enefit280 WHB ash studied here are not typically used for alkali activation, even though some studies [27–29] suggest that class C, i.e. high-Ca fly ashes, can be used for the production of geopolymeric binders. High CaO in the source material used for alkali activation can potentially strengthen the polymeric structures by providing extra nucleation sites for silicate through the formation of an amorphous Ca-Al silicate hydrate (C-A-S-H) gel [30]. In principle, the alkali elements ( $\text{Ca}^{2+}$ ,  $\text{Mg}^{2+}$ ,  $\text{Na}^+$ ,  $\text{K}^+$  or the so-called network modifying agents) present in fly ash provide charge balancing by balancing the negative charge of tetrahedral aluminium that forces the aluminium to stay in 4-coordination. Aluminium in 4-coordination has a higher solubility than the 6-coordination form, thus making more Al available for geopolymerization. Therefore the fly ashes with higher network modifying agents generally produce stronger geopolymers [31].

The Enefit280 WHB ash is characterized by a high content of alkali modifiers (Ca, Mg, K). However, there are not enough soluble silicate phases, which suggests that the extent of polymerization and the development of strength in the WHB ash are not limited by the availability of the network modifiers but by the lack of potentially soluble silica and specifically aluminum phases. As a result, even though the alkali activated WHB ash shows higher performance than the plain water hydrated WHB ash, the compressive strength of polymer composites is much lower than that typically achieved upon geopolymerization [32].

## 5. Conclusions

Until the present day the amount of ash residue coming from the Estonian shale oil industry has been relatively small. However, the shale oil producers in Estonia are shifting their focus to a new and more powerful type of solid heat carrier retorts, such as the Enefit280 retort. In the near future the share of oil production in the overall turnout of the Estonian oil shale industry should increase and, consequently, the amounts of waste ash residue generated would increase as well.

The current study shows that the Enefit280 waste heat boiler ash formed at low temperatures ( $< 800$  °C) contains a low concentration of reactive Ca-phases and the soluble amorphous (aluminium)-silicate phase/glass material and exhibits only limited self-cementing properties upon hydration

with plain water, with its uniaxial compressive strength reaching 3.8 MPa after 28 days of curing. Alkali activation of the WHB ash with a 5M NaOH solution resulted in the lack of significant hardening and an average compressive strength of 1 MPa was measured in the samples after 28 days. This kind of behaviour can be explained by the inhibition or suppressed formation of cementitious phases (as ettringite). The ash mixtures activated with Na-silicate and/or Na-silicate-NaOH mixtures show higher compressive strength values, indicating the formation of a Ca-Na-Al-silicate or C-S-H gel and reaching 11 MPa after 28 days of curing.

Overall, compared to other ash types forming in the Estonian oil shale processing technologies, the Enefit280 ash displays significantly lower self-cementing properties. This needs to be taken into account when designing waste depositories, if other types of ash with better self-cementing properties are not co-deposited with the Enefit280 ash.

### Acknowledgements

We wish to express our gratitude to Jaan Aruväli of Department of Geology, University of Tartu, for his help with testing and analysing the ash mixtures, as well as to Eesti Energia AS for providing the Enefit280 ash sample.

### REFERENCES

1. Liive, S. Oil shale energetics in Estonia. *Oil Shale*, 2007, **24**(1), 1–4.
2. Ots, A. *Oil Shale Fuel Combustion*. Tallinna Raamatutrükikoda, Tallinn, 2006.
3. Soone, J., Doilov, S. Sustainable utilization of oil shale resources and comparison of contemporary technologies used for oil shale processing. *Oil Shale*, 2003, **20**(3S), 311–323.
4. Mõtsep, R., Kirsimäe, K., Talviste, P., Puura, E., Jürgenson, J. Mineral composition of Estonian oil shale semi-coke sediments. *Oil Shale*, 2007, **24**(3), 405–422.
5. Golubev, N. Solid oil shale heat carrier technology for oil shale retorting. *Oil Shale*, 2003, **20**(3), 324–332.
6. Veiderma, M. Estonian oil shale – Resources and usage. *Oil Shale*, 2003, **20**(3S), 295–303.
7. Aarna, I. Developments in production of synthetic fuels out of Estonian oil shale. *Energ. Environ.*, 2011, **22**(5), 541–552.
8. Garcia-Lodeiro, I., Fernandez-Jimenez, A., Blanco, M. T., Palomo, A. FTIR study of the sol-gel synthesis of cementitious gels: C–S–H and N–A–S–H. *J. Sol-Gel Sci. Techn.*, 2008, **45**(1), 63–72.
9. Fernández-Carrasco, L., Torrens-Martín, D., Morales, L. M., Martínez-Ramírez, S. Infrared spectroscopy in the analysis of building and construction materials. In: *Infrared Spectroscopy – Materials Science, Engineering and Technology* (Theophanides, T., ed.), InTech, Rijeka, Croatia, 2012, 369–382.

10. Lodeiro, I. G., Macphee, D. E., Palomo, A., Fernandez-Jimenez, A. Effect of alkalis on fresh C–S–H gels. FTIR analysis. *Cement Concrete Res.*, 2009, **39**(3), 147–153.
11. Yu, P., Kirkpatrick, R. J., Poe, B., McMillan, P. F., Cong, X. D. Structure of calcium silicate hydrate (C–S–H): Near-, mid-, and far-infrared spectroscopy. *J. Am. Ceram. Soc.*, 1999, **82**(3), 742–748.
12. Rees, C. A., Provis, J. L., Lukey, G. C., van Deventer, J. S. J. In situ ATR-FTIR study of the early stages of fly ash geopolymer gel formation. *Langmuir*, 2007, **23**(17), 9076–9082.
13. Lecomte, I., Henrist, C., Liegeois, M., Maseri, F., Rulmont, A., Cloots, R. (Micro)-structural comparison between geopolymers, alkali-activated slag cement and Portland cement. *J. Eur. Ceram. Soc.*, 2006, **26**(16), 3789–3797.
14. Mõtlep, R., Sild, T., Puura, E., Kirsimäe, K. Composition, diagenetic transformation and alkalinity potential of oil shale ash sediments. *J. Hazard. Mater.*, 2010, **184**(1–3), 567–573.
15. Paaver, P., Paiste, P., Kirsimäe, K. Geopolymeric potential of the Estonian oil shale solid residues: Petroter solid heat carrier retorting ash. *Oil Shale*, 2016, **33**(4), 373–392.
16. Talviste, P., Sedman, A., Mõtlep, R., Kirsimäe, K. Self-cementing properties of oil shale solid heat carrier retorting residue. *Waste Manage. Res.*, 2013, **31**(6), 641–647.
17. Bitjukova, L., Mõtlep, R., Kirsimäe, K. Composition of oil shale ashes from pulverized firing and circulating fluidized-bed boiler in Narva Thermal Power Plants, Estonia. *Oil Shale*, 2010, **27**(4), 339–353.
18. Kuusik, R., Uibu, M., Kirsimäe, K., Mõtlep, R., Meriste, T. Open-air deposition of Estonian oil shale ash: Formation, state of art, problems and prospects for the abatement of environmental impact. *Oil Shale*, 2012, **29**(4), 376–403.
19. Uibu, M., Somelar, P., Raado, L.-M., Irha, N., Hain, T., Koroljova, A., Kuusik, R. Oil shale ash based backfilling concrete – strength development, mineral transformations and leachability. *Constr. Build. Mater.*, 2016, **102**, Part 1, 620–630.
20. Mindess, S., Young, J. F., Darwin, D. *Concrete*. 2nd ed. Prentice Hall, Pearson Education, Inc., Upper Saddle River, NJ, 2003.
21. Sedman, A., Talviste, P., Kirsimäe, K. The study of hydration and carbonation reactions and corresponding changes in the physical properties of co-deposited oil shale ash and semicoke wastes in a small-scale field experiment. *Oil Shale*, 2012, **29**(3), 279–294.
22. Sedman, A., Talviste, P., Mõtlep, R., Jõelett, A., Kirsimäe, K. Geotechnical characterization of Estonian oil shale semi-coke deposits with prime emphasis on their shear strength. *Eng. Geol.*, 2012, **131–132**, 37–44.
23. Anthony, E. J., Bulewicz, E. M., Dudek, K., Kozak, A. The long term behaviour of CFBC ash-water systems. *Waste Manage.*, 2002, **22**(1), 99–111.
24. Raado, L.-M., Hain, T., Liisma, E., Kuusik, R. Composition and properties of oil shale ash concrete. *Oil Shale*, 2014, **31**(2), 147–160.
25. Provis, J. L., Bernal, S. A. Alkali-activated binders – chemistry and engineering. *Rilem Proc.*, 2014, **92**, 299–327.
26. Clark, B. A., Brown, P. W. Formation of ettringite from monosubstituted calcium sulfoaluminate hydrate and gypsum. *J. Am. Ceram. Soc.*, 1999, **82**(10), 2900–2905.

27. Guo, X. L., Shi, H. S., Chen, L. M., Dick, W. A. Alkali-activated complex binders from class C fly ash and Ca-containing admixtures. *J. Hazard. Mater.*, 2010, **173**(1–3), 480–486.
28. Guo, X. L., Shi, H. S., Dick, W. A. Compressive strength and microstructural characteristics of class C fly ash geopolymer. *Cement Concrete Comp.*, 2010, **32**(2), 142–147.
29. Mijarsh, M. J. A., Johari, M. A. M., Ahmad, Z. A. Effect of delay time and  $\text{Na}_2\text{SiO}_3$  concentrations on compressive strength development of geopolymer mortar synthesized from TPOFA. *Constr. Build. Mater.*, 2015, **86**, 64–74.
30. Van Deventer, J. S. J., Provis, J. L., Duxson, P., Lukey, G. C. Reaction mechanisms in the geopolymeric conversion of inorganic waste to useful products. *J. Hazard. Mater.*, 2007, **139**(3), 506–513.
31. Aughenbaugh, K. L., Stutzman, P., Juenger, M. C. G. Assessment of the glassy phase reactivity in fly ashes used for geopolymer cements. In: *Geopolymer Binder Systems* (Struble, L., Hicks, J. K., eds.), Selected Technical Papers STP, **1566**, 2013, ASTM International, West Conshohocken, PA, 2013, 11–20.
32. Provis, J. L., Palomo, A., Shi, C. J. Advances in understanding alkali-activated materials. *Cement Concrete Res.*, 2015, **78**, Part A, 110–125.

Received January 10, 2017